

Original Article

Local bone interaction between renin-angiotensin system and kallikrein-kinin system in diabetic rat

Yong Li^{1*}, Guang-Si Shen^{2*}, Chen Yu², Guang-Fei Li², Jun-Kang Shen¹, You-Jia Xu², Jian-Ping Gong¹

Departments of ¹Radiology, ²Orthopaedics, The Second Affiliated Hospital of Soochow University, 1055 Sanxiang Road, Suzhou, China. *Equal contributors.

Received August 31, 2014; Accepted October 18, 2014; Epub February 1, 2015; Published February 15, 2015

Abstract: Objective: This study was performed to investigate bone deteriorations and the involvement of skeletal renin-angiotensin system (RAS) and kallikrein-kinin system (KKS) of male rat in response to the hyperglycemia. Methods: The biomarkers in serum and urine were measured by ELISA kit, and tibias were taken for the measurement on gene, protein expression and histological analysis, femurs were taken for the measurement on biomechanical parameters and micro-CT. Results: The DM1 showed the decreased level of osteocalcin, testosterone and FGF-23, and the increased level of serum CTX as compared to those of vehicle group. The H&E staining showed remarkable bone deteriorations, including increased disconnections and separation of trabecular bone among growth plate and joint cartilage in DM1 group. Biomechanically, the maximum load, maximum stress, and strain parameter of DM1 group was significantly lower than control group. Type 1 diabetic mice displayed bone loss shown the reduction of bone volume/total volume, trabecular number, trabecular thickness and bone mineral density. The STZ injection significantly up-regulated mRNA expression of AT1R, AGT, renin, renin-receptor, and ACE, and the expression of AT2R, B1R and B2R were down-regulated in tibia of rat in hyperglycemia group. The protein expression of renin, ACE and Ang II were significantly up-regulated, and AT2R, B1R and B2R were down-regulated in DM1 group. Conclusions: The treatment of hyperglycemia was detrimental to bone as compared to the vehicle group, and the underlying mechanism was mediated, at least partially, through down-regulation of KKS activity and up-regulation of RAS activity in local bone.

Keywords: Renin-angiotensin system, kallikrein-kinin system, hyperglycemia, bone

Introduction

The renin-angiotensin system (RAS) plays an important role in the regulation of the cardiovascular system and the kallikrein-kinin system (KKS) appears to counteract most of the RAS effects [1]. The RAS and the KKS each encompasses a large number of molecules that participate in many diverse aspects of physiology and pathophysiology such as angiogenesis [2, 3], insulin resistance [4, 5], atherosclerosis [6, 7], diabetic nephropathy [8, 9], and cardiac hypertrophy [10, 11]. Recent studies showed that tissue RAS or KKS can autonomic control in rats with overactivity [1, 12]. Moreover, plasma KKS assembly and activation can counterbalance the RAS activity [12]. Dramatically, angiotensin-converting enzyme (ACE) inhibitors influence the kallikrein-kinin system and report-

edly have immunomodulatory characteristics. Modulation of KKS by ACE inhibitor, enalapril, alleviates experimental autoimmune encephalomyelitis through up-regulation the expression of bradykinin. Additionally, bradykinin receptor antagonist administration reduced the favorable effects of enalapril [13]. All available evidence indicates that there are numerous interactions between the renin-angiotensin system and kallikrein-kinin system in local tissue.

Estrogen deficiency rat model revealed that Ang II could stimulate the differentiation and activity of osteoclasts in vivo. As a key active peptide in RAS, Ang II could accelerate osteoporosis of OVX rats [14]. Ang II has been shown to act on osteoblasts to stimulate the production of the osteoclastogenic cytokine, receptor activator of NF- κ B ligand (RANKL), thereby increasing the

differentiation of osteoclasts indirectly [15]. Moreover, the local RAS in bone was involved in age-related osteoporosis of aging mice [16], bone deterioration of mice with unilateral ureteral obstruction [17], and glucocorticoid-induced osteoporotic rabbit [18]. It was reported that hyperglycemia could lead to bone deteriorations due to the high activity of skeletal RAS [19]. However, whether the local interaction between RAS and KKS in bone is involved in the skeletal deteriorations associated with hyperglycemia is not known yet.

Studies in kininogen-deficient rats and B1 and B2 receptor gene knockout mice provide evidence for an important role for kinin peptides in the regulation of blood pressure and sodium homeostasis, renal response to vasopressin, insulin sensitivity, and in contributing to inflammatory processes [20]. There have been reports that B2 receptor and tissue kallikrein gene knockout mice develop cardiomyopathy, and that the tissue kallikrein gene knockout mice develop impaired flow-induced vasodilatation [21]. In mice knockout the bradykinin B1 receptor (*Bdkrb1* (-/-)), the results indicated that *Bdkrb1* (-/-) mice exhibiting increased bone loss. Bone marrow cells from *Bdkrb1* (-/-) displayed increased differentiation into functional osteoclasts with consistent artificial calcium phosphate degradation [22]. More than that, lack of B1R and B2R exacerbates diabetic complications such as renal injury and bone mineral loss [23]. Furthermore, the enhanced kinin B1 and B2 receptor expression induced by the pro-inflammatory cytokines might be involved in enhancing bone resorption [24].

We hypothesized that the local RAS and KKS in bone might be involved in the pathogenesis of hyperglycemia. Therefore, the aim of the present work was to investigate the interaction between RAS and KKS in bone which is involved in the skeletal deteriorations associated with type 1 diabetes mellitus (DM1) induced by streptozotocin (STZ).

Materials and methods

Animal treatment

Ten-week-old male Sprague-Dawley rats (Slac Laboratory Animal, Shanghai, China) were allowed to acclimate to the environment for 1 week. All experimental procedures were carried out in accordance with the guidelines of the Shanghai Science and Technology Council on

Animal Care. All chemicals and reagents were purchased from Sigma (Oakville, Ontario, Canada), except where noted.

The rats were randomly divided into two groups: (1) control group (n=10); (2) streptozotocin (STZ)-induced hyperglycemia rats (DM1, n=12). The animals were induced hyperglycemia by intraperitoneal injection of STZ, dissolved in citrate buffer (0.1 M at pH 4.5), at 60 mg/kg body weight with singly injection. The rats in control group were injected with solvent. All mice were sacrificed 8 weeks after STZ injection. The fasting blood glucose (FBG) levels were measured with a blood glucose monitoring system (Roche). Body weight and FBG were recorded every two weeks during experimental period. The animals were treated in accordance with the guidelines of the Animal Ethic Committee of The Second Affiliated Hospital of Soochow University.

Chemistries in serum and urine

The concentrations of calcium (Ca) and creatinine (Cr) from serum and urine were measured by standard colorimetric methods using a micro-plate reader (Bio-Tek, USA). The level of urine Ca was corrected by the concentration of urine Cr. Serum levels of testosterone, fibroblast growth factors-23 (FGF-23), osteocalcin and C-terminal telopeptide of type I collagen (CTX) were measured using ELISA kits (Immutopics, Inc., San Clemente, CA, USA) with ELISA reader (MD SpectraMax M5, USA).

Bone histology

The tibias were decalcified in 0.5 M EDTA (pH 8.0) and then embedded in paraffin by standard histological procedures. Section of 5 μ m were cut and stained with hematoxylin & eosin (H&E), and visualized under a microscope (Leica DM 2500).

The BMD of femurs were measured by dual-energy X-ray absorptiometry (DEXA) (LUNAR DPXIQ, GE Healthcare, USA). After DEXA measurements, the trabecular bone microarchitecture of the distal femoral metaphysis was measured using a microtomography scanner (Sky-Scan 1076, Kontizh, Belgium) with a slice thickness of 22 μ m. The volume of interest (VOI) was trabecular compartments based on 100 consecutive slices away from the distal femur growth plate. The 3D images were obtained for visualization and display. Bone morphometric

Table 1. Primers sequence used for RT-PCR analysis

Gene	Forward primer sequence (5' 3')	Reverse primer sequence (5' 3')
AT1R	CCATCACCAGATCAAGTGCA	TGGGGCAGTCATCTTGAATTCT
AT2R	ACTTCTCCCTTGCCACCATC	ATCTTATCCGATGGCTTATG
ACE	CCCATCTGCTAGGGAACATGT	GGTGTCCATCCCTGCTTTATCA
Renin	GAGGCCTTCCTTAGCCAATC	TGTGAATCCCACAAGCAAGG
Renin-receptor	CTTTAGCGAGGAGAGAGTGTAT	ATGTAGCACTTGCAGTTCGGAGAGA
AGT	CGAGTGGGAGAGGTTCTCAA	CTCGTAGATGGCGAACAGGA
B1R	GCATCCCCACATTCTTCTA	AAGAAGTGGTAAGGGCACCA
B2R	CTTGGGTGAGCTCAGTGCA	TAGGGGCAGACATTGAAGG
GAPGH	GGTGCTGAGTATGTCGTG	TTGAGCTCTGGGATGACC

mm/min until the femur fractured. The load, stress, and strain-deflection curves were automatically calculated by the computer using the Bluehill software. The femora were kept moist at all times during the testing. The parameters measured were load, stress, and strain.

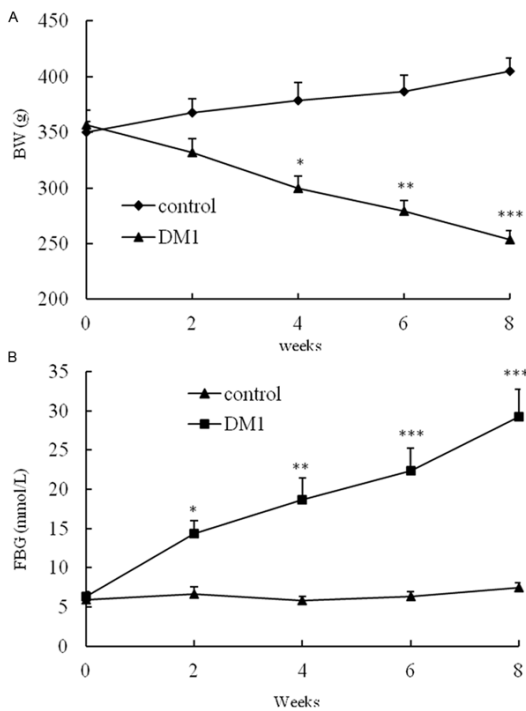


Figure 1. Body weight (BW) and fasting blood glucose (FBG) throughout the study. BW (A) and FBG (B) were recorded every two weeks during experimental period. Values are expressed as mean \pm SEM, n=10 in each group. * $P < 0.05$, ** $P < 0.01$, *** $P < 0.01$, versus control group.

parameters, including bone volume over total volume (BV/TV), trabecular number (Tb.N), and trabecular thickness (Tb.Th), were obtained by analyzing the VOI.

Biomechanical parameters

Femurs were placed on the Instron machine (Instron Microtester 5848, Instron Corp., USA) in a three-point bending configuration. The load was applied at the mid-diaphysis in an antero-posterior direction with a loading speed of 5

Real time-polymerase

chain reaction

The proximal tibia of each animal was crushed under liquid nitrogen conditions and RNA extraction was performed according to the TRIzol manufacturer's protocol (Invitrogen, Carlsbad, CA, USA). RNA integrity was verified by agarose gel electrophoresis. Synthesis of cDNAs was performed by reverse transcription reactions with 2 μ g of total RNA using moloney murine leukemia virus reverse transcriptase (Invitrogen) with oligo dT (15) primers (Fermentas) as described by the manufacturer. The first strand cDNAs served as the template for the regular polymerase chain reaction (PCR) performed using a DNA Engine (ABI 7300). Glyceraldehyde 3-phosphate dehydrogenase (GAPDH) as an internal control was used to normalize the data to determine the relative expression of the target genes. The reaction conditions were set according to the kit instructions. After completion of the reaction, the amplification curve and melting curve were analyzed. Gene expression values are represented using the $2^{-\Delta\Delta Ct}$ method. The PCR primers of the RAS and KKS components used in this study were shown in **Table 1**.

Western blotting

The proximal tibia were homogenized and extracted in NP-40 buffer, followed by 5-10 min boiling and centrifugation to obtain the supernatant. Samples containing 50 μ g of protein were separated on 10% SDS-PAGE gel, transferred to nitrocellulose membranes (Bio-Rad Laboratories, Hercules, CA, USA). After saturation with 5% (w/v) non-fat dry milk in TBS and 0.1% (w/v) Tween 20 (TBST), the membranes were incubated with the following antibodies, bradykinin B1 receptor (B1R), bradykinin B2 receptor (B2R), angiotensin II type 1 receptor

Local bone interaction between the RAS and KKS

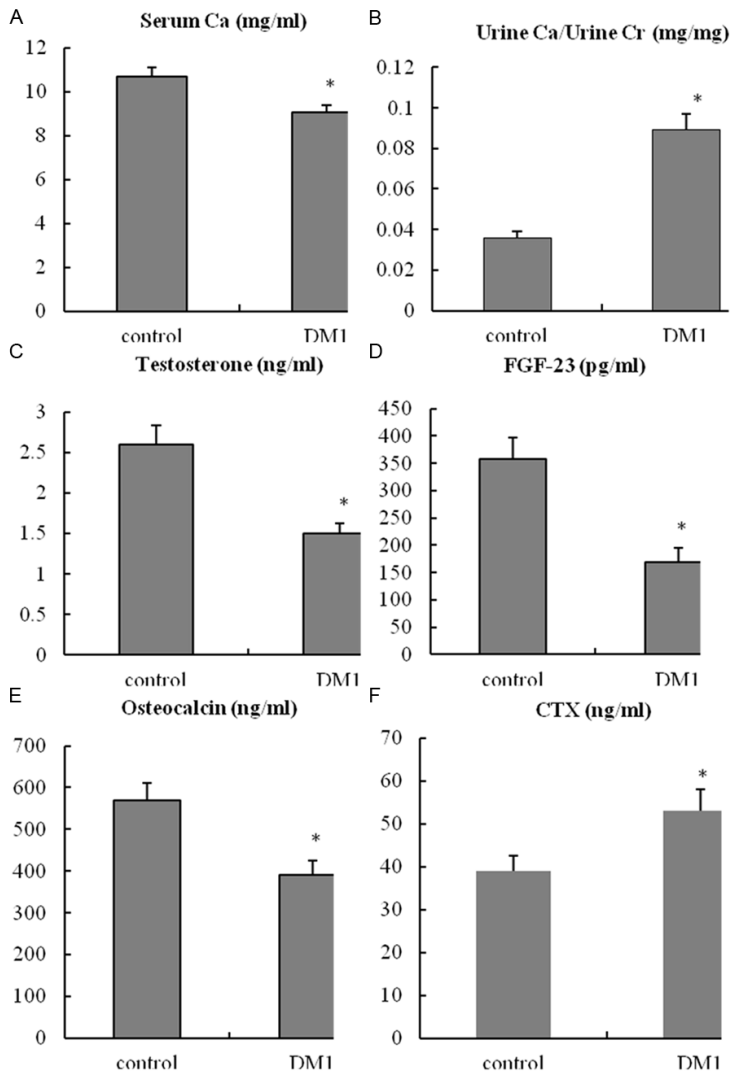


Figure 2. Biochemical parameters analysis of serum and urine. Serum calcium (Ca) (A), urine calcium (Ca) (B), testosterone (C), fibroblast growth factors-23 (FGF-23) (D), osteocalcin (E) and C-terminal telopeptide of type I collagen (CTX) (F). Values are expressed as mean \pm SEM, n=7-10 in each group. * $P < 0.05$, versus control group.

(AT1R), angiotensin II type 2 receptor (AT1R), angiotensin-converting enzyme (ACE), renin, renin-receptor (R-R), angiotensinogen (AGT) (Santa Cruz, USA), at dilutions ranging from 1:500 to 1:2,000 at 4°C over-night. After three washes with TBST, membranes were incubated with secondary immunoglobulins (Igs) conjugated to IRDye 800CW Infrared Dye (LI-COR), including donkey anti-goat IgG and donkey anti-mouse IgG at a dilution of 1:10,000-1:20,000. After 1 hour incubation at 37°C, membranes were washed three times with TBST. Blots were visualized by the Odyssey Infrared Imaging System (LI-COR Biotechnology). Signals were densitometrically assessed (Odyssey Application Sof-

ware version 3.0) and normalized to the β -actin signals to correct for unequal loading using the mouse monoclonal anti- β -actin antibody (Bioworld Technology, USA).

Statistical analysis

The data from these experiments were reported as mean \pm standard errors of mean (SEM) for each group. All statistical analyses were performed by using PRISM version 4.0 (GraphPad). Inter-group differences were analyzed by one-way ANOVA, and followed by Tukey's multiple comparison test as a post test to compare the group means if overall $P < 0.05$. Differences with P value of < 0.05 were considered statistically significant.

Results

Basic physiological and biochemical parameters

Four weeks after the STZ injection, the mean BW of the STZ-treated rat was significantly lower than that of the control group (**Figure 1A**). The FBG value of DM1 rats rose from 14 mmol/L at week 2 to 29 mmol/L at week 8. The FBG in the DM1 group was significantly increased compared to that of the vehicle group from week 2 to week 8 (**Figure 1B**).

The Ca level was determined in the serum and urine, decreased the serum Ca level and increased

urine Ca excretion as compared to those of vehicle group (**Figure 2A** and **2B**). Additionally, DM1 group showed significantly lower testosterone, FGF-23 and osteocalcin compared to vehicle group (**Figure 2C-E**). There was significant difference in the CTX levels between the vehicle and DM1 groups (**Figure 2F**).

Bone histology

Histological analysis on trabecular bone in proximal metaphysis of the tibia was performed by H&E staining (**Figure 3A** and **3B**). H&E staining showed the increased disconnections and separation of trabecular bone zone among growth plate and joint cartilage, and trabecular

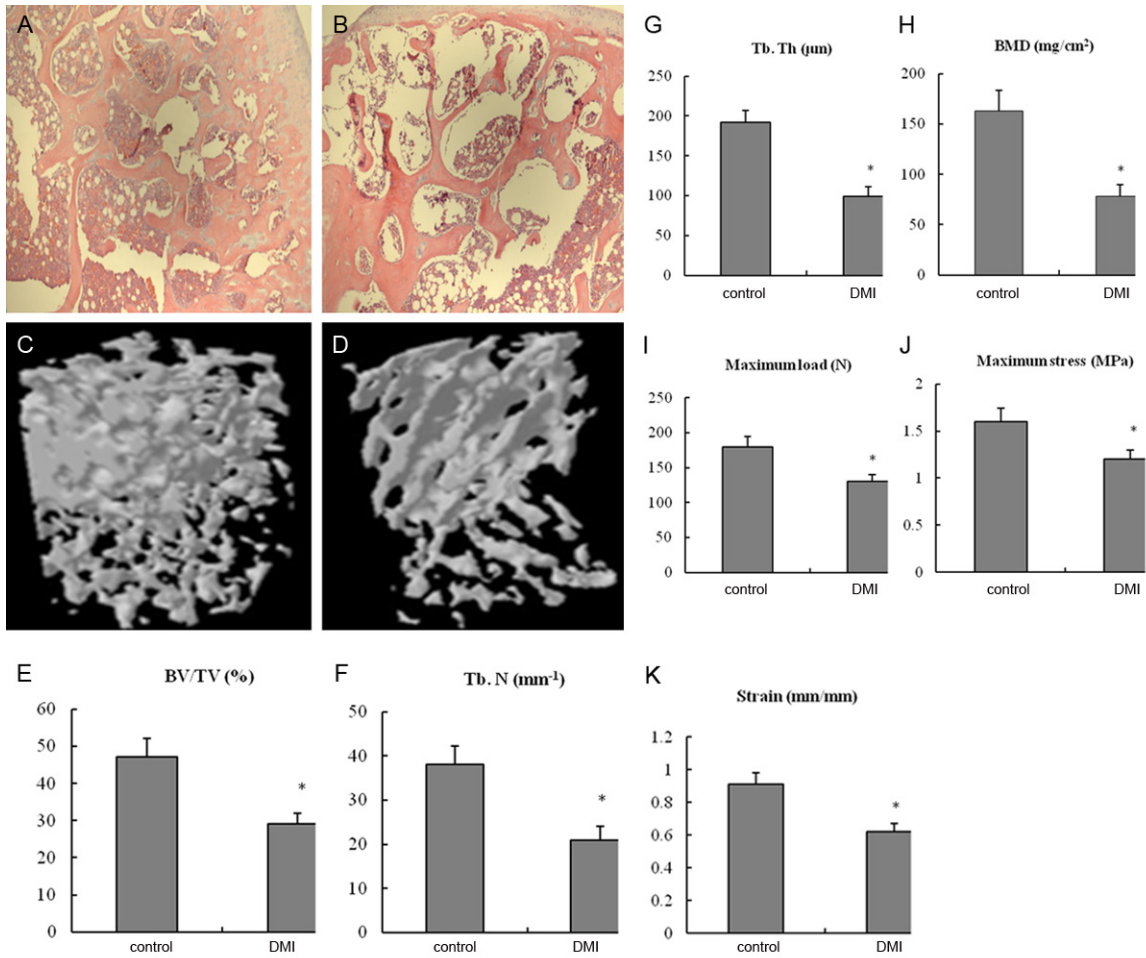


Figure 3. Histological staining, three-dimensional architecture and Biomechanical parameters. Hematoxylin and eosin staining of the proximal metaphysis of the tibia, trabecular bone zone among growth plate and joint cartilage region were shown (A and B). Three-dimensional architecture of trabecular bone within the distal femoral metaphyseal region of femurs (C and D), BV/TV the trabecular bone volume over total volume (E), Tb. N number of trabeculae (F), Tb. Th thickness of the trabeculae (G), and BMD bone mineral density (H). Biomechanical parameters of femur with maximum load values (I), maximum stress values (J) and Strain values (K). Values are expressed as mean ± SEM, n=5 in each group. *P < 0.05, versus control group.

bone network as well as the reduction of trabecular bone mass of primary and secondary spongiosa throughout the proximal metaphysis of tibia at DM1 group.

Micro-CT analysis and BMD

Three-dimensional images of the distal metaphysis of the femur with differences in the trabecular microarchitecture between the control group and DM1 group were presented in **Figure 3C** and **3D**. Furthermore, the decreased in BV/TV (**Figure 3E**), Tb.N (**Figure 3F**), and Tb.Th (**Figure 3G**) was significantly different between the DM1 group and the vehicle group. We also found that the femoral BMD values in DM1 group decreased significantly (**Figure 3H**).

Biomechanical parameters

As for the biomechanical parameters, there was significant difference between the vehicle and DM1 groups, the significantly lower maximum load (**Figure 3I**), maximum stress (**Figure 3J**), and strain (**Figure 3K**) parameters for the DM1 group compared to the vehicle group.

MRNA and protein expression of skeletal RAS and KKS components

The mRNA and protein expression of AT1R and ACE were significantly higher in proximal tibia of DM1 group than vehicle group (**Figure 4A, 4C, 4I** and **4J**). The mRNA expression of renin (**Figure 4D**), R-R (**Figure 4E**), AGT (**Figure 4F**)

Local bone interaction between the RAS and KKS

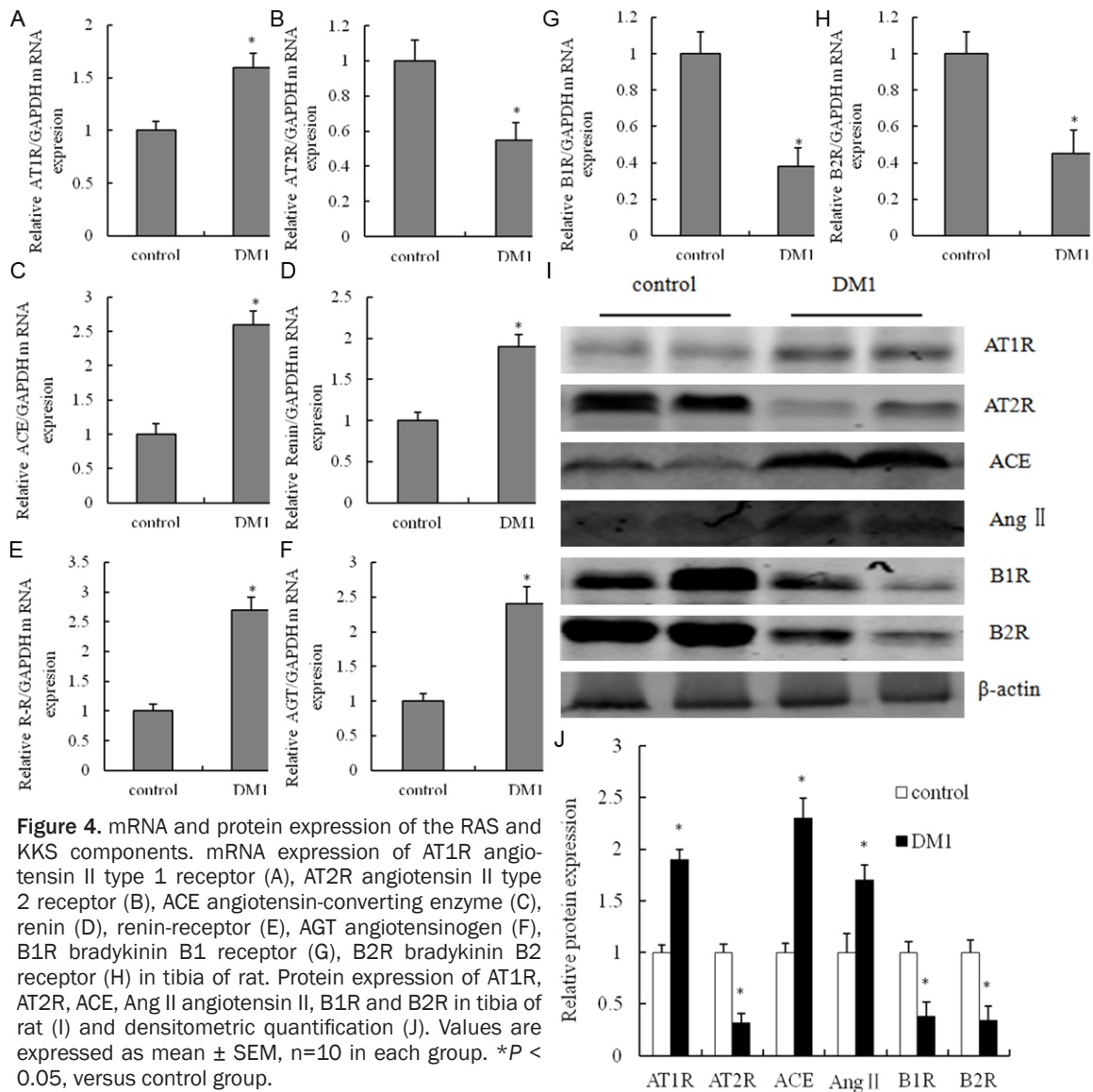


Figure 4. mRNA and protein expression of the RAS and KKS components. mRNA expression of AT1R angiotensin II type 1 receptor (A), AT2R angiotensin II type 2 receptor (B), ACE angiotensin-converting enzyme (C), renin (D), renin-receptor (E), AGT angiotensinogen (F), B1R bradykinin B1 receptor (G), B2R bradykinin B2 receptor (H) in tibia of rat. Protein expression of AT1R, AT2R, ACE, Ang II angiotensin II, B1R and B2R in tibia of rat (I) and densitometric quantification (J). Values are expressed as mean \pm SEM, n=10 in each group. * $P < 0.05$, versus control group.

and the protein expression of Ang II (**Figure 4I** and **4J**) were increased in DM1 group. Interestingly, STZ induction showed a tendency to down-regulate the mRNA and protein expression of AT2R, bradykinin B1 and B2 receptor (**Figure 4B** and **4G-J**), the knockout of which could induce bone deteriorations.

Discussion

Type 1 diabetes mellitus (DM1) results in hyperglycemia because of an absolute insulin insufficiency. This leads to many complications, both microvascular and macrovascular pathological changes [25]. Recent clinical surveys showed that DM1 elevates fracture risks of hip, vertebral, proximal humerus, tibia, wrist and ankle independent of BMD [26-29]. Moreover, DM1

has been recognized a relationship between diabetes, delayed healing of fractures and bone defects in animal models [19, 30]. Recent studies showed that bone tissue RAS or KKS play a vital role in bone deteriorations during hyperglycemia [19, 22, 23]. However, the pathological role of skeletal interaction between the RAS and KKS in bone deteriorations induced by hyperglycemia is not clearly known. Therefore, the present study was performed to investigate the possible pathological mechanism, from the view of skeletal interaction between RAS and KKS, involved in bone damages of hyperglycemia induced by streptozotocin (STZ) injection.

In this study STZ injection successfully led to hyperglycemia, 14 mmol/L < FBG, of rat in DM1

group. The STZ-induced increasing in bone resorption was confirmed by the increased level of CTX and the decreased level of osteocalcin in the serum, and the decreased level of serum Ca and the increased level of urinary Ca excretion. Moreover, histological staining also confirmed the results. A recently identified phosphatonin, known as fibroblast growth factor 23 (FGF-23), disclosed new pathways in the pathophysiology of mineral metabolism [31]. Clinical studies had shown that the downregulation of serum FGF-23 levels in Crohn disease appeared as a secondary compensatory effect on the bone and mineral metabolism induced by chronic intestinal inflammation [32]. This study provided evidence that the downregulation of serum FGF-23 levels in diabetic rat. Interestingly, we demonstrated that the decreased level of testosterone in the serum of rat in DM1 group. Clinical surveys showed that total osteocalcin was positively correlated with testosterone in male patients with T2DM, so total osteocalcin might predict the testosterone level in the serum [33]. In an aged orchidectomised rat model [34], testosterone replacement was able to raise the testosterone level and restore the bone volume of orchidectomised rats. We proposed that hyperglycaemia may tend to suppress testosterone level and enhance bone calcium loss and collagen degradation in type 1 diabetic rat.

We had analyzed the mRNA and protein expression of the RAS and KKS components, downregulation of KSS and up-regulation of RAS activity. In this study, clear evidence was provided for the existence of a cross-talk of RAS with KKS during bone deterioration involved in the development and progression of type 1 diabetes mellitus. The RAS and KKS interact at several aspects. Plasma kallikrein has been implicated in the activation of pro-renin [20]. Renin or/and pro-renin as a moderator could control RAS to start, and independent play to its own physiological function mediated by its receptor [35]. Moreover, kallikrein can cleave angiotensinogen to generate Ang II directly [20]. In addition to inhibition of bradykinin metabolism, ACE inhibitors potentiate the effects of bradykinin by a process dependent on cross talk between ACE and the B2 receptor [36]. Another example of interaction between the RAS and KKS is the formation of heterodimer between AT1 and B2 receptor; the heterodimer may contribute to the increased resistance of AT1 receptors to inactivation [37]. In this study,

we demonstrated that the expression of AT1R was up-regulated and the expression of B2R was down-regulated in tibia of mice in DM1 group. Further evidence of interaction between the RAS and KKS is the finding that the B2 receptor antagonist HOE 140 can prevent some of the consequences of AT1 receptor antagonism [38, 39], suggesting that bradykinin may mediate some of the effects of AT1 receptor antagonism. One possible mechanism is that activation of the AT2 receptor during AT1 receptor antagonism may lead to increased bradykinin formation [38]. Interestingly, in the present study, a treatment of hyperglycemia could obviously inhibit the expression of AT2R in tibia of rat in DM1 group.

Taken all together, our results identified that the hyperglycemia induced bone deteriorations performance in the three-dimensional structure degradation and biomechanical strength reduction. The underlying mechanism was mediated, at least partially, through down-regulation of KKS activity and up-regulation of RAS activity. Moreover, these studies will identify new potential therapeutic targets to treat diabetic complications.

Acknowledgements

This work was supported by Grants from the National Natural Science Foundation of China (81273090, 81302438), the Natural Science Foundation of Jiangsu Province (BK2012608), Research and Innovation Project for College Graduates of Jiangsu Province (CX10B_053Z), and the Foundation Program of Suzhou Key Laboratory of High Technology (SZS201208).

Disclosure of conflict of interest

None.

Address correspondence to: Dr. Jian-Ping Gong, Department of Radiology, 1055 Sanxiang Road, The Second Affiliated Hospital of Soochow University, Suzhou 200135, Jiangsu, P. R. China. Tel: (86) 512-65223693; Fax: (86) 512-65223693; E-mail: gongjianping_SAH@163.com

References

- [1] Ribeiro JM, Santos RA, Pesquero JB, Bader M and Krieger EM. Autonomic control in rats with overactivity of tissue renin-angiotensin or kallikrein-kinin system. *Regul Pept* 2005; 129: 155-159.

- [2] Mai J, Qiu Q, Lin YQ, Luo NS, Zhang HF, Wen ZZ, Wang JF and Yang X C. Angiotensin II-derived reactive oxygen species promote angiogenesis in human late endothelial progenitor cells through heme oxygenase-1 via ERK1/2 and AKT/PI3K pathways. *Inflammation* 2014; 37: 858-870.
- [3] Wright JK, Botha JH and Naidoo S. Influence of the kallikrein-kinin system on prostate and breast tumour angiogenesis. *Tumour Biol* 2008; 29: 130-136.
- [4] Fukushima A, Kinugawa S, Takada S, Matsu-shima S, Sobirin MA, Ono T, Takahashi M, Suga T, Homma T, Masaki Y, Furihata T, Kadoguchi T, Yokota T, Okita K and Tsutsui H. (Pro)renin Receptor in the Skeletal Muscle is Involved in the Development of Insulin Resistance Associated with Post-Infarct Heart Failure in Mice. *Am J Physiol Endocrinol Metab* 2014; [Epub ahead of print].
- [5] Potier L, Waeckel L, Fumeron F, Bodin S, Fysekidis M, Chollet C, Bellili N, Bonnet F, Gusto G, Velho G, Marre M, Alhenc-Gelas F, Rousset R and Bouby N. Tissue kallikrein deficiency, insulin resistance, and diabetes in mouse and man. *J Endocrinol* 2014; 221: 305-316.
- [6] Sridharan V, Tripathi P, Sharma SK, Moros EG, Corry PM, Lieblong BJ, Kaschina E, Unger T, Thone-Reineke C, Hauer-Jensen M and Boerma M. Cardiac inflammation after local irradiation is influenced by the kallikrein-kinin system. *Cancer Res* 2012; 72: 4984-4992.
- [7] Fraga-Silva RA, Savergnini SQ, Montecucco F, Nencioni A, Caffa I, Soncini D, Costa-Fraga FP, De Sousa FB, Sinisterra RD, Capettini LA, Lenglet S, Galan K, Pelli G, Bertolotto M, Pende A, Spinella G, Pane B, Dallegri F, Palombo D, Mach F, Stergiopoulos N, Santos RA and da Silva RF. Treatment with Angiotensin-(1-7) reduces inflammation in carotid atherosclerotic plaques. *Thromb Haemost* 2014; 111: 736-747.
- [8] Mori J, Patel VB, Ramprasath T, Alrob OA, Des-Aulniers J, Scholey JW, Lopaschuk GD and Oudit GY. Angiotensin 1-7 mediates renoprotection against diabetic nephropathy by reducing oxidative stress, inflammation, and lipotoxicity. *Am J Physiol Renal Physiol* 2014; 306: F812-821.
- [9] Tomita H, Sanford RB, Smithies O and Kakoki M. The kallikrein-kinin system in diabetic nephropathy. *Kidney Int* 2012; 81: 733-744.
- [10] Koyama S, Tsuruda T, Ideguchi T, Kawagoe J, Onitsuka H, Ishikawa T, Date H, Hatakeyama K, Asada Y, Kato J and Kitamura K. Osteoprotegerin is secreted into the coronary circulation: a possible association with the renin-angiotensin system and cardiac hypertrophy. *Horm Metab Res* 2014; 46: 581-586.
- [11] Batista EC, Batista EC, Ramalho JD, Reis FC, Barros CC, Moraes MR, Pesquero JL, Bacurau RF, Pesquero JB and Araujo RC. Swimming training exacerbates pathological cardiac hypertrophy in kinin B2 receptor-deficient mice. *Int Immunopharmacol* 2008; 8: 271-275.
- [12] Schmaier AH. The plasma kallikrein-kinin system counterbalances the renin-angiotensin system. *J Clin Invest* 2002; 109: 1007-1009.
- [13] Uzawa A, Mori M, Taniguchi J and Kuwabara S. Modulation of kallikrein-kinin system by the angiotensin-converting enzyme inhibitor alleviates experimental autoimmune encephalomyelitis. *Clin Exp Immunol* 2014; [Epub ahead of print].
- [14] Shimizu H, Nakagami H, Osako MK, Hanayama R, Kunugiza Y, Kizawa T, Tomita T, Yoshikawa H, Ogihara T and Morishita R. Angiotensin II accelerates osteoporosis by activating osteoclasts. *FASEB J* 2008; 22: 2465-2475.
- [15] Kaneko K, Ito M, Fumoto T, Fukuhara R, Ishida J, Fukamizu A and Ikeda K. Physiological function of the angiotensin AT1a receptor in bone remodeling. *J Bone Miner Res* 2011; 26: 2959-2966.
- [16] Gu SS, Zhang Y, Li XL, Wu SY, Diao TY, Hai R and Deng HW. Involvement of the skeletal renin-angiotensin system in age-related osteoporosis of ageing mice. *Biosci Biotechnol Biochem* 2012; 76: 1367-1371.
- [17] Gu SS, Zhang Y, Wu SY, Diao TY, Gebru YA and Deng HW. Early molecular responses of bone to obstructive nephropathy induced by unilateral ureteral obstruction in mice. *Nephrology (Carlton)* 2012; 17: 767-773.
- [18] Yongtao Z, Kunzheng W, Jingjing Z, Hu S, Jianqiang K, Ruiyu L and Chunsheng W. Glucocorticoids activate the local renin-angiotensin system in bone: possible mechanism for glucocorticoid-induced osteoporosis. *Endocrine* 2014; [Epub ahead of print].
- [19] Diao TY, Pan H, Gu SS, Chen X, Zhang FY, Wong MS and Zhang Y. Effects of angiotensin-converting enzyme inhibitor, captopril, on bone of mice with streptozotocin-induced type 1 diabetes. *J Bone Miner Metab* 2014; 32: 261-270.
- [20] Campbell DJ. The renin-angiotensin and the kallikrein-kinin systems. *Int J Biochem Cell Biol* 2003; 35: 784-791.
- [21] Campbell DJ. The kallikrein-kinin system in humans. *Clin Exp Pharmacol Physiol* 2001; 28: 1060-1065.
- [22] Goncalves-Zillo TO, Pugliese LS, Sales VM, Mori MA, Squaiella-Baptistao CC, Longo-Maugeri IM, Lopes JD, de Oliveira SM, Monteiro AC and Pesquero JB. Increased bone loss and amount of osteoclasts in kinin B1 receptor knockout mice. *J Clin Periodontol* 2013; 40: 653-660.
- [23] Kakoki M, Sullivan KA, Backus C, Hayes JM, Oh SS, Hua K, Gasim AM, Tomita H, Grant R,

Local bone interaction between the RAS and KKS

- Nossov SB, Kim HS, Jennette JC, Feldman EL and Smithies O. Lack of both bradykinin B1 and B2 receptors enhances nephropathy, neuropathy, and bone mineral loss in Akita diabetic mice. *Proc Natl Acad Sci U S A* 2010; 107: 10190-10195.
- [24] Brechter AB, Persson E, Lundgren I and Lerner UH. Kinin B1 and B2 receptor expression in osteoblasts and fibroblasts is enhanced by interleukin-1 and tumour necrosis factor-alpha. Effects dependent on activation of NF-kappaB and MAP kinases. *Bone* 2008; 43: 72-83.
- [25] Armas LA, Akhter MP, Drincic A and Recker RR. Trabecular bone histomorphometry in humans with Type 1 Diabetes Mellitus. *Bone* 2012; 50: 91-96.
- [26] Loureiro MB, Ururahy MA, Freire-Neto FP, Oliveira GH, Duarte VM, Luchessi AD, Brandao-Neto J, Hirata RD, Hirata MH, Maciel-Neto JJ, Arrais RF, Almeida MG and Rezende AA. Low bone mineral density is associated to poor glycemic control and increased OPG expression in children and adolescents with type 1 diabetes. *Diabetes Res Clin Pract* 2014; 103: 452-457.
- [27] Janghorbani M, Feskanich D, Willett WC and Hu F. Prospective study of diabetes and risk of hip fracture: the Nurses' Health Study. *Diabetes Care* 2006; 29: 1573-1578.
- [28] Vestergaard P, Rejnmark L and Mosekilde L. Relative fracture risk in patients with diabetes mellitus, and the impact of insulin and oral antidiabetic medication on relative fracture risk. *Diabetologia* 2005; 48: 1292-1299.
- [29] Patsch JM, Burghardt AJ, Yap SP, Baum T, Schwartz AV, Joseph GB and Link TM. Increased cortical porosity in type 2 diabetic postmenopausal women with fragility fractures. *J Bone Miner Res* 2013; 28: 313-324.
- [30] Rao Sirasanagandla S, Ranganath Pai Karkala S, Potu BK and Bhat KM. Beneficial Effect of *Cissus quadrangularis* Linn. on Osteopenia Associated with Streptozotocin-Induced Type 1 Diabetes Mellitus in Male Wistar Rats. *Adv Pharmacol Sci* 2014; 2014: 483051.
- [31] Razzaque MS. The FGF23-Klotho axis: endocrine regulation of phosphate homeostasis. *Nat Rev Endocrinol* 2009; 5: 611-619.
- [32] Oikonomou KA, Orfanidou TI, Vlychou MK, Kapsoritakis AN, Tsezou A, Malizos KN and Potamianos SP. Lower fibroblast growth factor 23 levels in young adults with Crohn disease as a possible secondary compensatory effect on the disturbance of bone and mineral metabolism. *J Clin Densitom* 2014; 17: 177-184.
- [33] Cui R, Su B, Sheng C, Cheng X, Yang P, Bu L, Li H, Wang J, Sheng H and Qu S. Total osteocalcin in serum predicts testosterone level in male type 2 diabetes mellitus. *Int J Clin Exp Med* 2014; 7: 1145-1149.
- [34] Tajul Ariff AS, Soelaiman IN, Pramanik J and Shuid AN. Effects of *Eurycoma longifolia* on Testosterone Level and Bone Structure in an Aged Orchidectomised Rat Model. *Evid Based Complement Alternat Med* 2012; 2012: 818072.
- [35] Castrop H, Hocherl K, Kurtz A, Schweda F, Todorov V and Wagner C. Physiology of kidney renin. *Physiol Rev* 2010; 90: 607-673.
- [36] Marcic BM and Erdos EG. Protein kinase C and phosphatase inhibitors block the ability of angiotensin I-converting enzyme inhibitors to resensitize the receptor to bradykinin without altering the primary effects of bradykinin. *J Pharmacol Exp Ther* 2000; 294: 605-612.
- [37] AbdAlla S, Lothar H, el Massiery A and Quitterer U. Increased AT(1) receptor heterodimers in preeclampsia mediate enhanced angiotensin II responsiveness. *Nat Med* 2001; 7: 1003-1009.
- [38] Liu YH, Yang XP, Sharov VG, Nass O, Sabbah HN, Peterson E and Carretero OA. Effects of angiotensin-converting enzyme inhibitors and angiotensin II type 1 receptor antagonists in rats with heart failure. Role of kinins and angiotensin II type 2 receptors. *J Clin Invest* 1997; 99: 1926-1935.
- [39] Katada J and Majima M. AT(2) receptor-dependent vasodilation is mediated by activation of vascular kinin generation under flow conditions. *Br J Pharmacol* 2002; 136: 484-491.